Methodology for the Identification of Systems with Non-linear Dynamic Behaviour

Marian Göllner[1*], Sven Jacobitz[1], Xiaobo Liu-Henke[1], Ludger Frerichs[2]

[1]Institute for Mechatronics, Ostfalia University of Applied Sciences,
Salzdahlumer Str. 46/48, D-38302 Wolfenbüttel; *mar.goellner@ostfalia.de*

[2]Institute for Mobile Machines and Commercial Vehicles, Technical University Braunschweig,
Langer Kamp 19a, D-38106 Braunschweig

SNE 35(3), 2025, 149-157, DOI: 10.11128/sne.35.tn.10745
Selected ASIM SST 2024 Postconf. Publication: 2024-12-10
Rec. Impr. English version: 2025-08-01; Accepted: 2025-08-15
SNE - Simulation Notes Europe, ARGESIM Publisher Vienna
ISSN Print 2305-9974, Online 2306-0271, www.sne-journal.org

Abstract. This paper investigates the identification and control of unstable, under-actuated systems with non-linear dynamic behaviour. Due to their instability and non-linear responses to conventional control techniques, these systems pose a particular challenge for precise modelling and effective control. To address these problems, we developed a methodical, model-based approach using rapid control prototyping (RCP), which is based on physical models and integrates model-in-the-loop (MiL), software-in-the-loop (SiL) and hardware-in-the-loop (HiL) testing. The methodological framework includes the identification of system dynamics using measurement data-based approaches and the verification of the models to ensure their accuracy. By applying these models to the specific example of the S-Mobile, a highly dynamic intralogistics system with a spherical electric drive, we demonstrate the effectiveness of the approach. The results show improved model accuracy and robust control of the system, emphasising its potential applicability in similarly complex technical systems.

Introduction and Problem Definition

The modelling and control of intelligent dynamic systems is a fundamental aspect of modern engineering. This task becomes particularly challenging when dealing with unstable, under-actuated systems with non-linear behaviour [1]. Such systems can be found in a variety of applications, from robotics to energy transmission systems, and require precise and reliable models for effective system design. In modern control engineering, the models used are of crucial importance. They are not only used for system design, but are an integral part of the controller functions. Lack of accuracy in modelling can lead to sub-optimal performance and even system failure. Therefore, the identification of system dynamics, especially in non-linear and under-actuated systems, is a key challenge. These systems are characterised by their tendency to respond to conventional control methods with unpredictable or unstable behaviour.

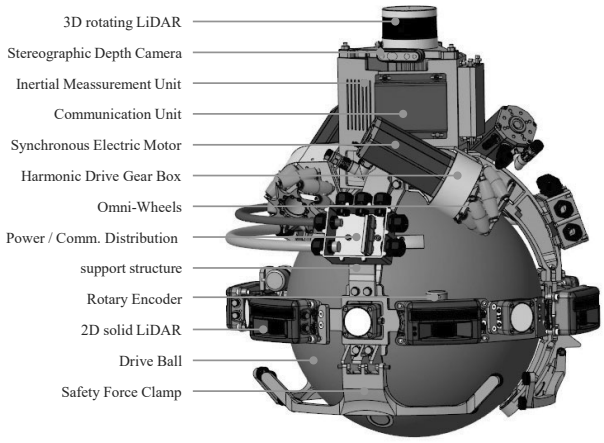

Figure 1: Function carrier S-Mobile as an exemplary non-linear, unstable system.

Figure 1 shows such a system, the S-Mobile function carrier, which is designed as a highly dynamic intralogistics system with a spherical electric drive. It consists of a structure that is balanced on a sphere via rotationally symmetrical actuators using omnidirectional wheels. The primary problem is the identification and validation of the control plant model as an integral part of the control concept (see [2]). The requirements for modelling quality are correspondingly high.

This paper presents the concept of a new methodology for the identification of unstable, underactuated systems taking into account there non-linear systems dynamic.

It is structured as follows. Section 1 introduces the methodology used for model-based development of mechatronic systems and the general model-based identification process.

Section 2 gives an overview over the state-of-the-art for identification of either non-linear or unstable systems. Subsequently, in section 3, the conception and design of the new method and in section 5, the results of the testing approach are laid out in detail. The paper closes in section 6 with a conclusion and an outlook for future work.

1 Methodology

A methodical, model-based approach is essential for the development of complex cyber-physical systems. Figure 2 illustrates the general data-based identification process used for this purpose, according to [3].

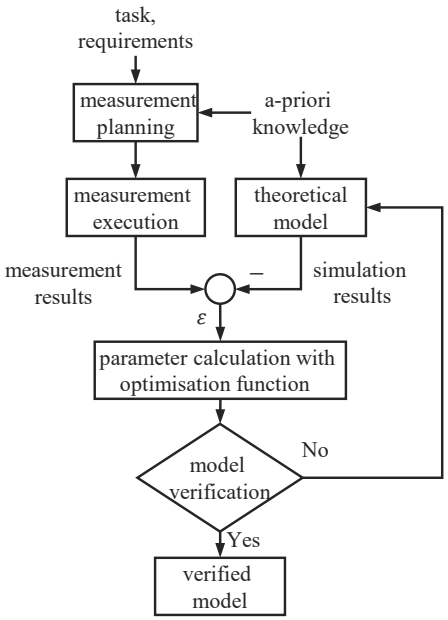

Figure 2: Measurement data-based model identification process.

Holistic, end-to-end, verification-orientated rapid control prototyping (RCP) has established itself as the defacto method in this area.

The core is a white-box model of the system to be controlled based on physical approaches as well as the processes model-in-the-loop (MiL), software-in-the-loop (SiL) and hardware-in-the-loop (HiL). The correctness of the model used is therefore an essential prerequisite for efficient development and valid design results. Model identification and verification are therefore core elements of the modelling process [4].

Based on the task, the requirements and the a-priori knowledge of the system, the measurement is first planned and the parameters of the theoretical model are initially estimated. The difference between the measurement and simulation results ε is used as input for an optimisation function to calculate the parameters. During model verification, an assessment is made as to whether the real behaviour is reproduced with sufficient accuracy. If this is the case, the final model is established. Otherwise, the theoretical model is adapted, for example by increasing the modelling depth.

2 State-of-the Art

Identification in control engineering refers to the experimental determination of the time behaviour of a process or system by analysing measured signals. The aim is to map the system behaviour as accurately as possible within a defined class of mathematical models, whereby the errors between the real process or system and its mathematical models should be minimised. The challenge is to keep the error between the actual system behaviour and its mathematical model as small as possible. Researchers and engineers use measured input and output signals to characterise and model the system dynamics. This process is crucial for the development of precise and efficient control systems, especially in technical fields such as robotics, aerospace and industrial automation, where accurate models are essential for optimal performance [5].

2.1 Classification of identification methods

Identification methods for dynamic systems can be fundamentally divided into two categories according to their basis of analysis: Time domain methods and frequency domain methods [6]. Time domain methods use time series data to characterise the dynamic behaviour of the system. These methods are particularly useful for modelling non-linear relationships between input and output signals [5].

In contrast, frequency domain methods analyse the system behaviour by examining the response of the system to sinusoidal input signals of different frequencies. These methods are effective in determining the system characteristics by analysing the frequency response. Frequency domain methods are particularly suitable for identifying linear systems as they provide a clear and descriptive representation of the system dynamics in the frequency spectrum [7].

In addition, there is a third category, the so-called mixed methods, which combine elements of both approaches in order to utilise the advantages of time and frequency domain analyses. These hybrid approaches are often able to provide a more comprehensive analysis by capturing both the direct time response and the frequency-dependent properties of the system [1].

The methods mentioned in the discussion above assume that the input/output behaviour of a system is measured directly. However, this approach is not practical for unstable systems. In such cases, the use of advanced techniques such as Closed Loop Identification is required [8]. When investigating under-actuated systems, it is also crucial to ensure that all system states are fully excited and analysed.

2.2 Approaches for the identification of non-linear, unstable systems

Current research in the field of system identification provides a wide range of perspectives on the challenges and methods for analysing dynamic systems, especially with the use of artificial intelligence and machine learning [8]. A common approach is to close the control loop to stabilise the system. A distinction is made here between direct (evaluation of the system input and output) and indirect (evaluation of the reference variable and the system output) identification methods. These methods make it possible both to create consistent models and to deal with non-modelled dynamics (approximate modelling) [9]. Xavier et al. [10] provide an in-depth overview.

In the specific application to underactuated systems, Chawla and Singla [11] apply adaptive neural-based fuzzy inference systems (ANFIS). Here, the model of an inverse pendulum is generated from input/output data of the dynamic system response. The accuracy of the ANFIS model is confirmed both by the mean square error and by experimental comparisons with real system models. However, this is a non-physics-based model, which is not suitable for treatment with typical control engineering methods.

Through Chen et al. [12] introduced dual input-output parameterisation (dual IOP), a new method for identifying linear time-invariant systems using closed-loop measurement data. The method represents an extension of previous approaches to closed-loop identification and simplifies the design of the stabilising controller in particular. The applicability for non-linear systems is not discussed.

Finally, González et al. [13] deal with the identification of unstable, continuous systems using refined instrumental variable methods, especially in closed-loop control. It is shown that existing approaches such as the Simplified Refined Instrumental Variable Method (SRIVC) in their conventional form are not reliable when it comes to modelling unstable systems.

As a solution, an adaptation of these methods is proposed, which includes the introduction of a specially adapted all-pass filter in the pre-filtering step. These modified methods allow the identification of unstable systems and minimise the error at convergence. However, the presented method is only intended to be applied to linear systems.

3 Designing the New Method

In order to be able to run through the established model-based design process and, in particular, to parameterise and use model-integrating control methods, an in-depth physical analysis of the system states and parameters is required. To do this, it is necessary to set up a physical model with fully defined parameters of the controlled system [14].

For this purpose, a modelling method based on balance equations taking into account conservation laws is to be favoured. According to Noether's theorem, every continuous symmetry of the effect results in a conservation law, and conversely, every conservation law has a continuous symmetry of the effect. This means that the underlying physics is fundamentally captured in the model and not obscured by approximation. This results in non-linear models with parameters that can be derived entirely from physics.

However, as mentioned at the beginning, the identification of these is non-trivial due to the non-linearity and possibly time variance. The method described below, which can in principle be carried out for any type of system in any domain, sequentially describes the targeted identification of system parameters using a mechanical system.

3.1 General model description

Based on the kinematics and dynamics of the respective mechanical system to be identified, the dynamics functions must first be derived in the form of coupled, non-linear differential equations. The following equation shows the generalised dynamics model [2] derived from this:

$$\underline{\underline{M}}\left(\underline{q}\right)\cdot\ddot{\underline{q}}+\underline{\underline{C}}\left(\underline{q},\dot{\underline{q}}\right)\cdot\dot{\underline{q}}+\underline{G}\left(\underline{q}\right)=\underline{\underline{F}}\left(\underline{q}\right)\cdot\underline{u} \qquad (1)$$

The symmetric mass matrix $\underline{\underline{M}}\in\mathbb{R}^{m\times m}$ depends on the individual masses of the systems' rigid bodies and the generalised coordinates $\underline{q}\in\mathbb{R}^m$. The vector $\underline{\underline{C}}\in\mathbb{R}^{m\times m}$ describes the generalised gyroscopic forces consisting of the centrifugal and Coriolis forces. The vector $\underline{G}\in\mathbb{R}^m$ describes the potential energy via gravity. The manipulated variables entered are calculated with the time-varying vector $\underline{u}\in\mathbb{R}^n$. Its multiplication with the functional matrix $\underline{\underline{F}}\in\mathbb{R}^{m\times n}$ leads to the torque matrix.

3.2 Linearisation of the model

Characteristics of the system dynamics from equation (1) can be analysed particularly well in the frequency range. To do this, a linear model is first required at different operating points. For example, a Taylor series expansion using Jacobian matrices can be used at different time steps i. The linearised model at the current operating point is corresponding:

$$\Delta\ddot{\underline{q}}=\underbrace{\left(-\underline{\underline{J}}_{\ddot{q}}(i)^{-1}\cdot\underline{\underline{J}}_{q}(i)\right)\cdot\Delta\underline{q}+\left(-\underline{\underline{J}}_{\ddot{q}}(i)^{-1}\cdot\underline{\underline{J}}_{\dot{q}}(i)\right)\cdot\Delta\dot{\underline{q}}}_{\text{for }\underline{\underline{A}}_i\cdot\underline{x}}$$
$$+\underbrace{\left(-\underline{\underline{J}}_{\ddot{q}}(i)^{-1}\cdot\underline{\underline{J}}_{u}(i)\right)\cdot\Delta\underline{u}}_{\text{for }\underline{\underline{B}}_i\cdot\underline{u}}+\underbrace{\left(-\underline{\underline{J}}_{\ddot{q}}(i)^{-1}\right)\cdot f\Big|_{AP_i}}_{\text{for }\underline{\underline{E}}_i\cdot\underline{z}_i}$$

The result is a linear state space model according to the following equation (2).

$$\begin{aligned}\dot{\underline{x}}&=\underline{\underline{A}}_i\cdot\underline{x}+\underline{\underline{B}}_i\cdot\underline{u}+\underline{\underline{E}}_i\cdot\underline{z}_i\\ \underline{y}&=\underline{\underline{C}}\cdot\underline{x}+\underline{\underline{D}}\cdot\underline{u}\end{aligned} \qquad (2)$$

3.3 Stabilisation of the system

Based on the state space representation valid for the operating point, the system should now be stabilised by at least a narrow validity range around the operating point i using state feedback.

A feedback gain $\underline{\underline{K}}$, which forms the control vector $\underline{u}$ via the simple control law $\underline{u}^T=-\left(\underline{\underline{K}}^T\cdot\underline{x}\right)^T=-\underline{x}^T\cdot\underline{\underline{K}}^T$ through the state feedback, results from various approaches to state control and does not have to be optimally designed but must be known and constant. The system gain is normalised and the control vector is transformed using a set-point-filter $\underline{\underline{N}}$. This results in the control law of the controller:

$$\underline{u}=-\underline{\underline{K}}_i\cdot\underline{x}+\underline{\underline{N}}_i\cdot\underline{w} \qquad (3)$$

From the point of view of the setpoint input $\underline{w}$, the closed control loop now reacts like a stable multivariable system within the physical limits defined mainly by manipulated variable limits. The system limits must be checked in the same way as the BIBO stability.

This is given by a consideration of the controllability; if $\left(\underline{\underline{A}},\underline{\underline{B}}\right)$ is completely controllable, the inherent dynamics can be set arbitrarily, ergo the system can also be stabilised.

3.4 Transfer-function and decoupling of the system

The system, which has now been stabilised by control, is to be decoupled for identification in the coordinate system of the rigid body (BCS) to be investigated and the independent transfer paths are to be represented as transfer-functions.

This provides access to the main diagonal of the transfer matrix of the overall system via the transfer functions $\frac{\vartheta_x}{\vartheta_{x\_set}}$, $\frac{\vartheta_y}{\vartheta_{y\_set}}$, $\frac{\vartheta_z}{\vartheta_{z\_set}}$ in the respective spatial directions (either rotatory or translatory).

The linear equivalent state space of the system has the manipulated variables τ_1,τ_2,τ_3 of the actuators as input vector $\underline{u}(t)$, since the effect of the manipulated variables in the system model is already taken into account in relation to the BCS.

The transfer-matrix $\underline{\underline{G}}_S(s)$ of the system can be obtained from the state space representation by transforming it into the Laplace-domain.

$$\underline{\underline{G}}_S(s)=\frac{\underline{X}(s)}{\underline{U}(s)}=\left(s\cdot\mathbb{I}-\underline{\underline{A}}\right)^{-1}\cdot\underline{\underline{B}} \qquad (4)$$

This system can now be divided into the system-representation in the BCS spatial direction $\underline{\underline{G}}_{S\_R}$ and a transformation of the manipulated variables using the transformation matrix $\underline{\underline{T}}$.

In the same way, the closed control loop can be utilised by applying the control law $\underline{u} = -\underline{\underline{K}} \cdot \underline{x} + \underline{\underline{N}} \cdot \underline{w}$ onto the state space representation.

$$\begin{aligned} \dot{\underline{x}}(t) &= \underline{\underline{A}} \cdot \underline{x}(t) + \underline{\underline{B}} \cdot \left(-\underline{\underline{K}} \cdot \underline{x}(t) + \underline{\underline{N}} \cdot \underline{w}(t) \right) \\ &\circ\!\!-\!\!\bullet \\ \underline{X}(s) \cdot \left(s \cdot \mathbb{I} - \underline{\underline{A}} + \underline{\underline{B}} \cdot \underline{\underline{K}} \right) &= \underline{\underline{B}} \cdot \underline{\underline{N}} \cdot \underline{W}(s) \end{aligned} \tag{5}$$

The Transfer matrix of the closed control loop in the reference case thus becomes:

$$\underline{\underline{G}}_W(s) = \frac{\underline{X}(s)}{\underline{W}(s)} = \left(s \cdot \mathbb{I} - \underline{\underline{A}} + \underline{\underline{B}} \cdot \underline{\underline{K}} \right)^{-1} \cdot \underline{\underline{B}} \cdot \underline{\underline{N}} \tag{6}$$

The state controller and the set-point-filter also consist of a component $\underline{\underline{K}}_R$ and $\underline{\underline{N}}_R$ acting in the spatial directions and the transformation of the manipulated variables to the actuator positions by the inverse transformation matrix $\underline{\underline{T}}^{-1}$.

In the Laplace-domain, this can be expressed by the transfer-matrices $\underline{\underline{K}}(s)$ and $\underline{\underline{N}}(s)$ or $\underline{\underline{K}}_R(s) = \underline{\underline{T}} \cdot \underline{\underline{K}}(s)$ and $\underline{\underline{N}}_R(s) = \underline{\underline{T}} \cdot \underline{\underline{N}}(s)$ of the controller and set-point-filter. The controlled system can be reshaped for observation in the spatial directions [15].

3.5 Identification of the system dynamics in the frequency domain

Since the system behaviour has so far only been derived theoretically from physical modelling, the transmission behaviour of the system is now to be identified by frequency response measurements on the real plant. Because the system to be identified is unstable, the reference transfer function of the system stabilised by a linear controller is first identified and the transfer behaviour of the uncontrolled system is calculated from this. As the calculation of a frequency response is only applicable to linear systems, the model linearised at a suitable operating point is used for identification.

This model should be adapted to the measured frequency response by varying the parameters. Only as few free parameters as possible should be used. The transfer behaviour of the controller and set-point-filter is known and results from the control parameters used in the measurement. The transfer function of the actuator should first be identified separately by a frequency response measurement so that it can be assumed to be known when identifying the reference transfer function.

The actuator-transfer-matrix then corresponds to the control-transfer-matrix of the manipulated-variable-control in the BCS (X- Y- and Z-direction):

$$\underline{\underline{G}}_{M\_R}(s) = \underline{\underline{T}} \cdot \begin{bmatrix} G_{m1}(s) & 0 & 0 \\ 0 & G_{m2}(s) & 0 \\ 0 & 0 & G_{m3}(s) \end{bmatrix} \cdot \underline{\underline{T}}^{-1} \tag{7}$$

This leads to a further possibility of representing the transfer-matrix in the referencing-case with the separated transfer-functions in relation to the BCS:

$$\begin{aligned} \underline{\underline{G}}_W(s) = \left(\mathbb{I} + \underline{\underline{G}}_{S\_R}(s) \cdot \underline{\underline{G}}_{M\_R}(s) \cdot \underline{\underline{K}}_R(s) \right)^{-1} \cdot \ldots \\ \cdot \underline{\underline{G}}_{S\_R}(s) \cdot \underline{\underline{G}}_M(s) \cdot \underline{\underline{N}}_R(s) \end{aligned} \tag{8}$$

This yields to the correspondig matrix form:

$$\underline{\underline{G}}_W(s) = \begin{bmatrix} \underline{\underline{G}}_{W_{\mathrm{Rot}}}(s) & \underline{\underline{G}}_{W_{\mathrm{Trans} \mapsto \mathrm{Rot}}}(s) \\ \underline{\underline{G}}_{W_{\mathrm{Rot} \mapsto \mathrm{Trans}}}(s) & \underline{\underline{G}}_{W_{\mathrm{Trans}}}(s) \end{bmatrix} \tag{9}$$

Here, the separated transfer matrices for the reference case describe the couplings of the rotational and translational degrees of freedom in the BCS, e.g. explicitly for the rotational degrees of freedom:

$$\underline{\underline{G}}_{W_{\mathrm{Rot}}}(s) = \begin{bmatrix} \frac{\Theta_x(s)}{\Theta_{x_{\mathrm{soll}}}(s)} & \frac{\Theta_x(s)}{\Theta_{y_{\mathrm{soll}}}(s)} & \frac{\Theta_x(s)}{\Theta_{z_{\mathrm{soll}}}(s)} \\ \frac{\Theta_y(s)}{\Theta_{x_{\mathrm{soll}}}(s)} & \frac{\Theta_y(s)}{\Theta_{y_{\mathrm{soll}}}(s)} & \frac{\Theta_y(s)}{\Theta_{z_{\mathrm{soll}}}(s)} \\ \frac{\Theta_z(s)}{\Theta_{x_{\mathrm{soll}}}(s)} & \frac{\Theta_z(s)}{\Theta_{y_{\mathrm{soll}}}(s)} & \frac{\Theta_z(s)}{\Theta_{z_{\mathrm{soll}}}(s)} \end{bmatrix} \tag{10}$$

If the two reference transfer matrices are equalised, the transfer matrix of the uncontrolled system can be deduced by identifying them and subtracting the known transfer matrices of the state controller and any prefilter as well as the previously measured and transformed transfer matrix of the actuator. By equating the eq. (6) with eq. (7), it is also possible to draw conclusions about the dynamics-matrix defined at the operating point and the input-matrix of the state space and to identify individual, unknown parameters of the system within the coefficients formed by the system parameters.

3.6 Pseudo-linear identification of the stabilised system plant

Since the uncontrolled and thus also the controlled system is non-linear, the amplitude of the excitation has an influence on the system behaviour, as these do not fundamentally fulfil the amplification and superposition principle [16].

Frequency response measurements are therefore carried out with different excitation amplitudes in order to investigate this influence.

Typical non-linearities of mechanical systems are e.g. friction in the form of Coulumb or Stribeck friction, force transmission breakdown, dependencies of system states e.g. on the gravity vector/velocity vector and variable coefficients [15]. Since these effects within the frequency spectrum are dependent on both the excitation amplitude and the excitation frequency, the measurement must be carried out in partial frequency bands and then combined into one measurement using the evaluation of coherence.

Basically, the structure of the physical model is used to simulate an expected frequency response using known parameters. The simulated curve of the amplitude and phase response $(A_{\mathrm{mod}}(\omega)_{dB}, \varphi_{\mathrm{mod}}(\omega))$ is compared with the curve of the measurement graph $(A_{\mathrm{meas}}(\omega)_{dB}, \varphi_{\mathrm{meas}}(\omega))$. The difference between simulation and measurement is represented as the Root Mean Square Error ε of both the amplitude difference $\Delta A(\omega)_{dB} = A_{\mathrm{meas}}(\omega)_{dB} - A_{\mathrm{mod}}(\omega)_{dB}$ and phase difference $\Delta\varphi(\omega) = \varphi_{\mathrm{meas}}(\omega) - \varphi_{\mathrm{mod}}(\omega)$ points and is calculated using the coherence-dependent weighting factor k_{eval}.

$$\varepsilon = \varepsilon_{mag} + \varepsilon_{phase}$$

$$\varepsilon_{mag} = \frac{1}{n}\left(\sum_{\omega=\omega_{\min}}^{\omega_{\max}} (\Delta A(\omega)_{dB})^2 \cdot k_{eval}(\omega)\right)$$

$$\varepsilon_{phase} = \frac{1}{n}\left(\sum_{\omega=\omega_{\min}}^{\omega_{\max}} (20 \cdot \log(1 + |\Delta\varphi(\omega)|))^2 \cdot k_{eval}(\omega)\right)$$

The actual identification of the unknown model parameters is carried out by optimising this error surface initialised via estimates, using a modified downhill simplex algorithm according to Nelder and Mead [5].

4 Used Test Bench Infrastructure

To validate the concept described, the test bench shown in Figure 3 was set up in which the S-Mobile function carrier introduced in section can be tested under safe and reproducible conditions.

In this test rig, the S-Mobile is restrained in a reconfigurable commissioning frame, which allows either blocking or limiting the degrees of freedom of the superstructure without inhibiting the degrees of freedom of the ball.

The test carrier is fixed by wire ropes of a defined length in such a way that a tilting movement up to a maximum angle is permitted. This allows the structure to be stabilised by a translational movement of the geometric centre of the sphere while at the same time preventing it from tilting.

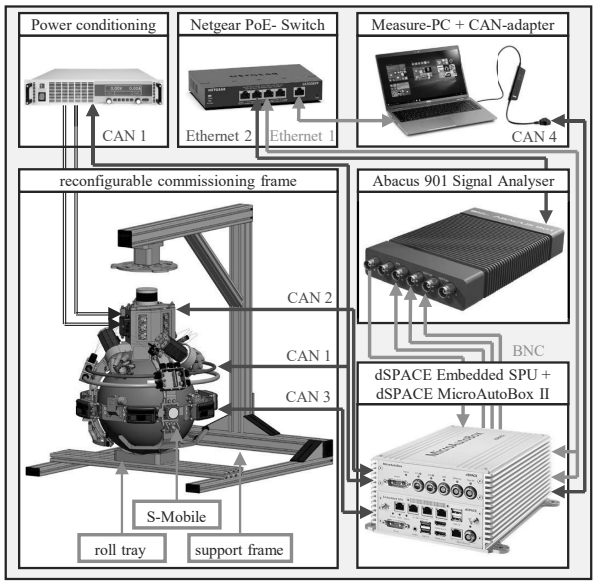

Figure 3: S-Mobile in test bench setup for identification.

The information technology linking of the measuring and control devices required for identification is also shown. The MicroAutoBox II as the RCP system of the S-Mobile is used to execute the linear stabilisation controller required for identification. The DP Abacus 901 signal analyser is coupled exclusively with this in order to specify the target variables for the stabilisation controller and to be able to calculate the delay time of the calculation duration of the control algorithm synchronously on all measurement channels.

Accordingly, all measurement signals required for identification are routed via the MicroAutoBox II. The signal measurement is not only carried out directly, but also by measurement data fusion algorithms that are mainly executed on the internally coupled embedded SPU. The actuators and sensors of the function carrier are connected via a real-time CAN network. Experiment preparation, remote ECU control and data recording are carried out on a measurement PC that communicates with both the MicroAutoBox II and the DP Abacus 901 via an Ethernet network.

5 Exemplary Application of the Method on the S-Mobile

Using the test bench presented in the previous chapter, frequency-dependent analyses were carried out on the S-Mobile function carrier. For this purpose, target states in the form of periodic excitations were given to the stabilisation controller as reference variables. The response of the closed control loop, consisting of the controller and system as well as the actuator and sensors, was then analysed.

The periodic excitations were selected on a system-specific basis in order to take specific non-linearities into account. For example, the amplitude of the excitation has an influence on the system behaviour. Frequency response measurements are therefore carried out with different excitation amplitudes in a fixed frequency range in order to investigate this influence. For excitation, amplitudes from $\hat{\vartheta}_{x\_\mathrm{set}} = 1.5°$ to $\hat{\vartheta}_{x\_\mathrm{set}} = 5°$ are fed in as chirp signals.

Figure 4 shows the recorded response spectra as a frequency response in the Bode diagram.

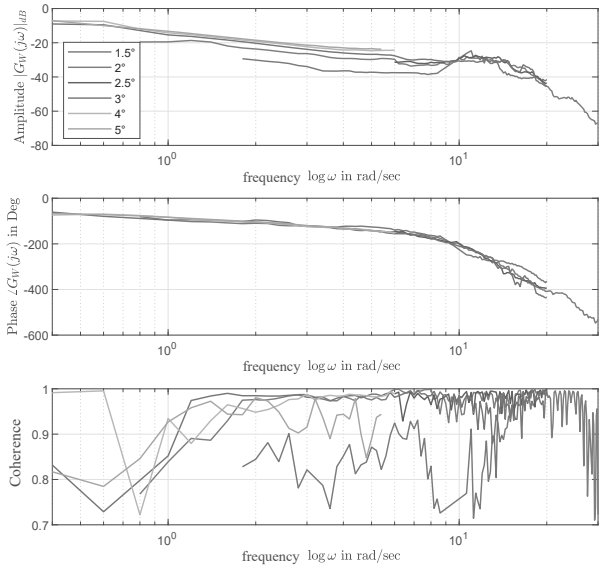

Figure 4: Measured frequency responses at different amplitude excitations, filtered by coherence.

Measurement series with a coherence of at least 0.7 across the entire spectrum have already been selected here. It can be seen that the coherence of the measurement starts to deteriorate significantly from approx. $20Hz$. This is due to the data transmission via CAN bus system from the RCP system to the actuators as well as from the sensors. The actual body angles were measured by an inertial measuring unit and transmitted via CAN with a cycle time of 10 ms. This corresponds to a sampling frequency of $100Hz$, whereby the Nyquist–Shannon sampling theorem [17] theoretically results in a maximum sampling frequency of 50Hz. In practice, however, the reconstructed signal is already distorted at lower frequencies, which results in a lower coherence of the signals. At higher amplitudes, the frequency response could only be determined for low frequencies, as excitation with a high frequency and high amplitude causes the wheels to slip due to the limited power distribution, thereby damaging the surface of the sphere.

The amplitude responses for large excitation amplitudes are close together, while the system for small excitations at low frequencies ($< 10Hz$) has a low gain and also poorer coherence. This is due to the large influence of static friction in the system at such low excitation amplitudes. The phase response, on the other hand, shows fewer deviations for all measurements.

The optimum parameters are identified by minimising the quadratic error between an assumed transfer-element as the reference-transfer-function of the separated transfer path within the transfer-matrix and the measured frequency response. Since both the transfer-function of the actuator and the transfer-functions of the controller (and set-point-filter) are known, the calculated reference model can be used to identify the structure of the transfer-element. This can also be estimated by observing the measured amplitude- and phase-drop.

To identify the parameters, the system transfer function $G_{sx}(s) = \frac{\theta_x(s)}{M_x(s)}$ must first be obtained by linearising the non-linear model with the mass moment of inertia as a free parameter. The model is to be linearised at the quasi-stable point $(\vartheta_x = 0, \vartheta_y = 0)$, as the system oscillates around this point during the frequency response measurement. However, the angular velocity is not assumed to be $\dot{\vartheta}_x = 0$ for the linearisation, but should correspond to the actual angular velocity during the measurement. However, this is not constant during the measurement, but depends on the frequency and amplitude of the oscillation. With a harmonic input oscillation $\vartheta_x(t)$ as the excitation signal, the angular velocity results from the following equation:

$$\vartheta_x(t) = A(\omega) \cdot \hat{\vartheta}_{x\_\mathrm{set}} \cdot \sin(\omega \cdot t + \varphi(\omega))$$

$$\dot{\vartheta}_x(t) = \frac{d\vartheta_x(t)}{dt} = A(\omega) \cdot \hat{\vartheta}_{x\_\mathrm{set}} \cdot \omega \cdot \cos(\omega \cdot t + \varphi(\omega))$$

For the zero crossing at the quasi-stable point around which the system oscillates ($\vartheta_x(t) = 0$), the maximum angular velocity results:

$$\dot{\vartheta}_x(\omega) = A(\omega) \cdot \hat{\vartheta}_{x\_\text{set}} \cdot \omega \tag{11}$$

The following figure 5 shows the maximum angular velocities associated with the measured frequency response.

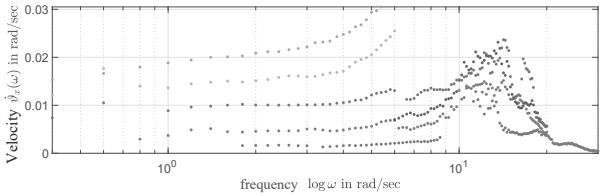

Figure 5: Angular velocity at zero crossing.

These are used for the linearisation of the reference model in order to derive the transfer-matrix using the method described in chapter 3. This in turn shows the structure and the parameter dependency, which can now be resolved according to an unknown parameter. By linearising the non-linear model at the operating point under consideration, for example, a system transfer function dependent on the moment of inertia θ_x can be derived in order to identify this as a free parameter via quadratic optimisation:

$$G_{sx}(s) = \frac{\vartheta_x(s)}{\tau_x(s)} = f(\sigma, \omega, \theta) \tag{12}$$

In combination with the known/identified actuator (-system) and the transfer-functions of the controller, the reference-transfer-function for the examined degree of freedom can be formed. The transfer-function of the state-feedback always results as a PDn-element, since the state controller always feeds back all minimum coordinates and at least their first derivative [18]. Furthermore, a dead time T_t is added to the transfer-element, which results from the data communication process.

$$G_w(s) = \frac{\vartheta_x(s)}{\vartheta_{x\_\text{set}}(s)} = \frac{N_{Rx} \cdot G_{sx}(s) \cdot G_m(s)}{1 + G_{sx}(s) \cdot G_m(s) \cdot K_{Rx}(s)} \cdot e^{-T_t \cdot s}$$

The frequency response of the applied transfer element with free initialised parameters is shown in green in the following figure 6. Quadratic optimisation results in the red curve after parameter adjustment. By minimising the error of the amplitude- and phase-response in relation to the measurement, unknown values for the free parameters of the example system were identified. A comparison with the design data of the system confirms the accuracy of the identified mass moment of inertia $\theta_x = 20.31$. This method can therefore be used to identify unknown parameters on under-actuated, unstable and non-linear systems.

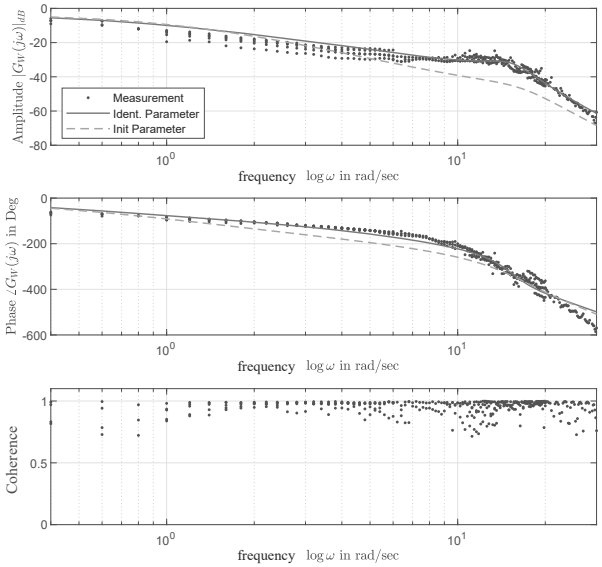

Figure 6: Identified transfer element for the command case.

6 Conclusions and Future Work

This paper discussed the identification and control of unstable, under-actuated systems with non-linear dynamic behaviour. The focus was on the development and validation of a new methodological procedure for system identification. Using the example of the S-Mobile, an innovative intralogistics system, it was successfully demonstrated how the system dynamics can be precisely identified and the system stabilised by applying the new approach.

For future work, further investigation of the approach is recommended in order to cover an even wider range of unstable, under-actuated systems. In particular, the integration of advanced machine learning methods and surrogate models [19] could further improve the accuracy and increase the adaptivity of the control systems. It would also be of great interest to investigate the transferability of the developed methods to other industrial applications to test their universal applicability.

Acknowledgement

This contribution was funded by the Lower Saxony Ministry of Science and Culture under grant number ZN3495 within the Lower Saxony "Vorab" of Volkswagen Foundation and supported by the Center for Digital Innovations (ZDIN).

Publication Remark

This contribution is the revised English version of the (German) conference version published in
Tagungsband Langbeiträge ASIM SST 2024,
ARGESIM Report AR 47,
ISBN ebook: 978-3-903347-65-6,
volume DOI 10.11128/arep.47,
article DOI 10.11128/arep.47.a4723, p 175-183.

References

[1] Schoukens J, Ljung L. Nonlinear System Identification: A User-Oriented Road Map. *IEEE Control Systems*. 2019;39(6):28–99.

[2] Liu-Henke X, Göllner M, Tao H. An intelligent control structure for highly dynamic driving of a spherical electrical drive. In: *2017 Twelfth International Conference on Ecological Vehicles and Renewable Energies (EVER)*. Piscataway, NJ: IEEE. 2017; pp. 1–10.

[3] Liu-Henke X, Jacobitz S, Göllner M, Scherler S, Yarom OA, Zhang J. A Holistic Methodology for Model-based Design of Mechatronic Systems in Digitized and Connected System Environments. In: *ICSOFT 2021*. [Setúbal, Portugal]: SCITEPRESS - Science and Technology Publications. 2021;.

[4] Gevers M. Identification for Control: From the Early Achievements to the Revival of Experiment Design*. *European Journal of Control*. 2005;11(4-5):335–352.

[5] Isermann R, Münchhof M. *Identification of Dynamic Systems*. Berlin, Heidelberg: Springer Berlin Heidelberg. 2011.

[6] Ljung L. Frequency Domain Versus Time Domain Methods in System Identification – Revisited. In: *Control of uncertain systems: modelling, approximation, and design*, edited by Francis BA, vol. 329 of *Lecture notes in control and information sciences*, pp. 277–291. Berlin and Heidelberg: Springer. 2006;.

[7] Pintelon R, Schoukens J. *System Identification: A Frequency Domain Approach*. Wiley. 2012.

[8] Nelles O. *Nonlinear System Identification: From Classical Approaches to Neural Networks, Fuzzy Models, and Gaussian Processes*. Cham: Springer International Publishing, 2nd ed. 2020.

[9] van den Hof P. Closed-loop issues in system identification. *Annual Reviews in Control*. 1998; 22:173–186.

[10] Xavier J, Patnaik SK, Panda RC. Process Modeling, Identification Methods, and Control Schemes for Nonlinear Physical Systems – A Comprehensive Review. *ChemBioEng Reviews*. 2021;8(4):392–412.

[11] Chawla I, Singla A. ANFIS based system identification of underactuated systems. *International Journal of Nonlinear Sciences and Numerical Simulation*. 2020;21(7-8):649–660.

[12] Chen R, Srivastava A, Yin M, Smith RS. Closed-Loop Identification of Stabilized Models Using Dual Input-Output Parameterization.

[13] González RA, Rojas CR, Pan S, Welsh JS. Refined instrumental variable methods for unstable continuous-time systems in closed-loop. *International Journal of Control*. 2023;96(10):2527–2541.

[14] Isermann R. *Mechatronische Systeme*. Berlin, Heidelberg: Springer Berlin Heidelberg. 2008.

[15] Göllner M, Liu-Henke X, Frerichs L. Analyse und Simulation des Kraftübertragungsverhaltens von Mecanum-Rädern. In: *Proceedings ASIM SST 2020*, edited by Deatcu C, Lückerath D, Ullrich O, Durak U, ASIM Mitteilung, pp. 89–98. Wien: ARGESIM Verlag. 2020;.

[16] Wittenburg J. *Dynamics of multibody systems*. Berlin and New York: Springer, 2nd ed. 2008.

[17] Seibt P. *Algorithmic Information Theory: Mathematics of Digital Information Processing*. Signals and communication technology. s.l.: Springer-Verlag, 1st ed. 2006.

[18] Karrenberg U. *Signale – Prozesse – Systeme*. Berlin, Heidelberg: Springer Berlin Heidelberg. 2017.

[19] Göllner M, Yarom OA, Fritz J, Liu-Henke X. Rechenzeitoptimierte Modellierung nicht-linearer physikalischer Prozesse mit Surrogate Modellen zur Anwendung in echtzeitfähigen Optimierungsverfahren. In: *Virtueller ASIM Workshop 2021*, edited by Liu-Henke X, Durak U, ASIM Mitteilung. Vienna: ARGESIM Verlag. 2021;.